ELSEVIER

Journal of Organometallic Chemistry 565 (1998) 49–62

Journal of Organometallic Chemistry

Reaction of ethynediyl, butadiynediyl and ethynyl iron complexes, $(\eta^5\text{-}C_5R_5)(CO)_2Fe\text{–}(C{\equiv}C)_n\text{–}X$ [$X = Fe(\eta^5\text{-}C_5R_5)(CO)_2$, H; $R_5 = Me_5$, Me_4Et; $n = 1, 2$], with $Fe_2(CO)_9$ leading to polynuclear C_2 and C_4 complexes[1]

Munetaka Akita *, Min-Chul Chung, Masako Terada, Masanori Miyauti, Masako Tanaka, Yoshihiko Moro-oka

Research Laboratory of Resources Utilization, Tokyo Institute of Technology, 4259 Nagatsuta, Midori-ku, Yokohama 226-8503, Japan

Received 17 November 1997

Abstract

Polynuclear C_2 and C_4 cluster compounds are prepared by treatment of the iron complexes containing μ-C_2 (ethynediyl), μ-C_4 (butadiynediyl) and C_2H (ethynyl) ligands with $Fe_2(CO)_9$. The ethynediyl complex $(\eta^5\text{-}C_5Me_5)(CO)_2Fe\text{–}C{\equiv}C\text{–}Fe(\eta^5\text{-}C_5Me_5)(CO)_2$ gives the tetrairon dicarbide complex, $(\mu_4\text{-}C_2)Fe_4(\eta^5\text{-}C_5Me_5)_2(CO)_9$, which shows dynamic behavior by way of reversible scission and recombination of the Fe–Fe bonds. Reaction of the butadiynediyl complex, $(\eta^5\text{-}C_5Me_5)(CO)_2Fe\text{–}C{\equiv}C\text{–}C{\equiv}C\text{–}Fe(\eta^5\text{-}C_5Me_5)(CO)_2$, affords tetranuclear nona- and decacarbonyl cluster compounds depending on the reaction conditions. The nonacarbonyl cluster compound formed exclusively in benzene adopts a normal acetylide cluster type structure and one of the two C≡C functional groups remains unreacted, but the decacarbonyl cluster isolated as a minor product from the reaction in THF consists of a μ_3-η^3-propargylidene diiron core and a ketene functional group, which should be formed by addition of an Fe_2 unit followed by migration of CO to the terminal carbon atom of the C_4 bridge. In contrast, reactions of polyynyl complexes are found to be less selective. Reaction of $(\eta^5\text{-}C_5Me_5)(CO)_2Fe\text{–}C{\equiv}C\text{–}H$ results in the formation of a low yield mixture of products, of which the *p*-quinone complex, *c*-2,5-$[Fe(\eta^5\text{-}C_5Me_5)(CO)_2]_2\text{–}C_6H_2O_2$, has been isolated and characterized by X-ray crystallography, though $(\eta^5\text{-}C_5Me_5)(CO)_2Fe\text{–}C{\equiv}C\text{–}C{\equiv}C\text{–}H$ merely gives an intractable reaction mixture. © 1998 Elsevier Science S.A. All rights reserved.

Keywords: Cluster compounds; Dicarbide; Polyynediyl complexes

1. Introduction

Transition metal polyynediyl complexes [M–$(C{\equiv}C)_n$–M] and polyynyl complexes [M–$(C{\equiv}C)_n$–H] have attracted much attention [1–3], because the π-system of the polycarbon linkage [–$(C{\equiv}C)_n$–] is extended to the metal termini through pπ–dπ conjugation. Such highly conjugated electronic system can stabilize unusual species (e.g. odd-electron species resulting from a redox process) and often shows unique properties (e.g. hyperpolarizability) [4]. In addition to this aspect, they have been recognized as versatile starting compounds for polynuclear complexes with polycarbon ligands (C_n) and studies on such complexes are of particular importance for comprehension of the interaction modes of polycarbon species with metal surfaces [5]. The C≡C parts are known to form π-bonds with transition metal species and further interaction of the added metal centers with the metal termini originally σ-bonded to the C_n rod often leads to the formation of cluster com-

* Corresponding author. E-mail: makita@res.titech.ac.jp

[1] Dedicated to Prof. Michael Bruce on the occasion of his 60th birthday in recognition of his important contribution to organometallic chemistry.

PII S0022-328X(98)00442-2

pounds. In our laboratory, systematic synthesis of polynuclear C2 complexes derived from the ethynediyl [M–C≡C–M] and ethynyl complexes [M–C≡C–H] [$n = 1$; M = Fe(η^5-C_5R_5)$(CO)_2$; R = H, Me] has been a subject of recent study, and a variety of cluster compounds have been obtained successfully [6]. The C2 cluster compounds can be viewed as model compounds for 'dicarbide' species. Now our study is being extended to C4 system.

Herein we disclose the results of the interaction of the ethynediyl– and butadiynediyl–diiron complexes, (η^5-C_5R_5)$(CO)_2$Fe–$(C{\equiv}C)_n$–Fe(η^5-C_5R_5)$(CO)_2$ [$n = 1$ (**1**), 2 (**2**); $R_5 = Me_5$, Me_4Et], and the ethynyl– and butadiynyl–iron complexes, (η^5-C_5R_5)$(CO)_2$Fe–$(C{\equiv}C)_n$–H [$n = 1$ (**3**), 2 (**4**)] ([6]p), with the diiron species $Fe_2(CO)_9$. The reaction of organic acetylenes with $Fe_2(CO)_9$ has been found to be rather complicated [7] compared to the selective reaction with $Co_2(CO)_8$ giving μ-η^2:η^2-adducts and, therefore, a mixture of various products are usually obtained depending on the reaction conditions and the structure of the acetylenic substrates. However, we have found that reaction with the ynediyl complexes **1** and **2** is selective.

2. Results and discussion

*2.1. Interaction of ethynediyl complex **1** with $Fe_2(CO)_9$: formation of a tetranuclear complex which exhibits dynamic behavior by way of reversible M–M bond scission and recombination*

Treatment of the ethynediyl complexes **1a** (C_5Me_5 derivative) and **1b** (C_5Me_4Et derivative) with $Fe_2(CO)_9$ at ambient temperature gave black precipitates **5a** and **5b** in 50 and 57% yields, respectively, after chromatographic separation of [Fe(η^5-C_5R_5)$(CO)_2$]$_2$ (Eq. 1).

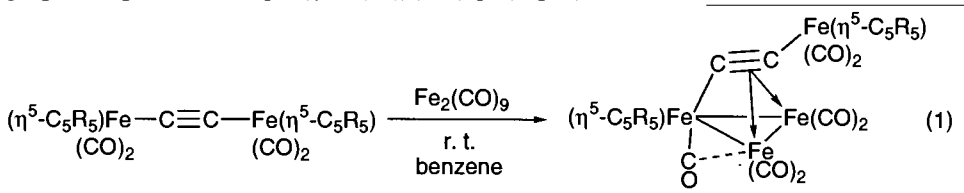

However, because the isolated, microcrystalline C_5Me_5 derivative **5a** was sparingly soluble in organic solvents, spectroscopic and structural analyses were performed for the C_5Me_4Et derivative **5b**. Since the IR features (KBr) of the CO stretching vibrations of **5a** and **5b** were essentially identical, the following discussion on the structure should hold true for both of the complexes.

The very broad ^{1}H-NMR spectrum of **5b** observed at room temperature (r.t.) did not provide us any structural information and then the solid state structure was determined by X-ray crystallography (Fig. 1 and Table 1). Because the isolated Fe(η^5-C_5Me_4Et)$(CO)_2$ moiety (Fe4) which does not interact with the triiron part apparently works as a substituent of the acetylide ligand, the tetrairon dicarbide complex **5b** is characterized as a triiron μ_3-η^1:η^2:η^2-acetylide cluster compound. The C1–C2 part [1.292(9) Å] is slightly elongated upon interaction with the two iron centers [cf. C≡C in **1b**: 1.206(6), 1.211(6) Å)] ([6]p). The coordination of the Fe(η^5-C_5Me_4Et)$(CO)_2$–C≡C moiety to the Fe_3 triangle is not symmetrical as can be seen from a top view (Fig. 2). The distances from the π-coordinated Fe centers to C2 are 2.224(8) Å (from Fe2) and 1.953(8) Å (from Fe3), and the former interatomic distance is in the upper limit of Fe–C bonding interaction. Another structural feature is the semi-bridging CO ligand [C11–O11; Fe1–C11–O11: 159.5(9)°], which is also indicated by the CO stretching vibration in the lower energy region (1850 cm^{-1}). The semi-bridging interaction makes the coordination structure of the Fe_3 core unsymmetrical. Detailed discussion as compared with related compounds will be described below.

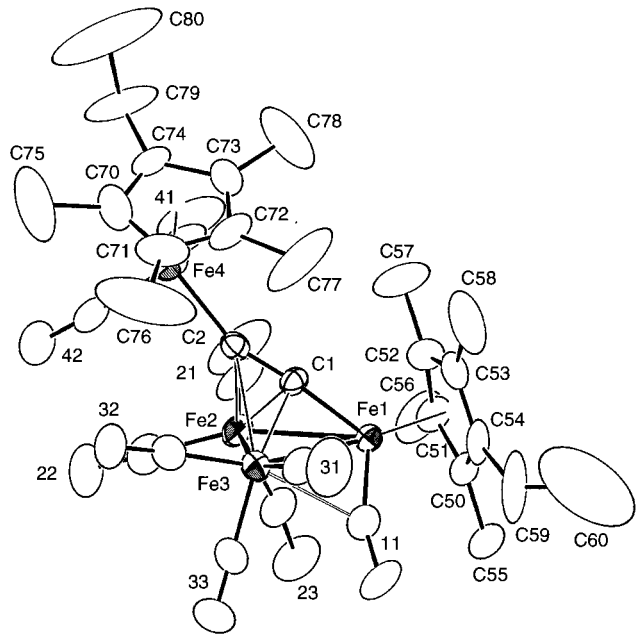

Fig. 1. Molecular structure of **5b** drawn at the 30% probability level. Labels without atom names are for the CO ligands.

Table 1
Comparison of the structural parameters for the core parts of **5b**, **10**, and **11**

5b		**10**		**11**[a]	
Interatomic distances (Å)					
Fe1–Fe2	2.610(2)	Co1–Fe2	2.604(1)	Fe4–Fe3	2.612(2)
Fe1–Fe3	2.642(2)	Co1–Fe3	2.600(1)	Fe1–Fe4	2.650(2)
Fe2–Fe3	2.524(2)	Fe2–Fe3	2.499(2)	Fe1–Fe3	2.516(1)
Fe1–C	1.829(7)	Co1–C2	1.856(6)	Fe4–C1	1.804(7)
Fe2–C1	1.996(7)	Fe2–C1	2.238(5)	Fe3–C1	2.034(8)
Fe2–C2	2.224(8)	Fe2–C2	1.990(5)	Fe3–C2	2.096(7)
Fe3–C1	1.995(8)	Fe3–C1	2.290(6)	Fe1–C1	2.001(8)
Fe3–C2	1.953(8)	Fe3–C2	2.002(6)	Fe1–C2	2.080(7)
Fe1–C11	1.75(1)	Fe–CO	1.741–1.785(8)	Fe1–C11	1.79(1)
Fe3–C11	2.40(1)	Co–CO	1.777–1.824(8)	Fe3–C11	2.250(9)
C11–O11	1.17(1)	Fe–C–O	1.138–1.163(9)	C11–O11	1.16(1)
Fe–Co[b]	1.72–1.83	Co–C–O	1.122–1.126(8)	Fe–CO[b]	1.77–1.81(1)
C–O[b]	1.11–1.17	—	—	C–O[b]	1.12–1.15(1)
C1–C2	1.292(9)	C1–C2	1.259(7)	C1–C2	1.311(9)
—	—	—	—	C2–C3	1.372(9)
—	—	—	—	C3–C4	1.231(9)
C2–Fe	1.953(8)	C1–Fe1	1.940(6)	C4–Fe2	1.900(7)
Bond angles (°)					
Fe2–Fe1–Fe3	57.46(6)	Fe2–Co1–Fe3	57.41(4)	Fe3–Fe4–Fe1	57.12(4)
Fe1–Fe2–Fe3	61.90(6)	Co1–Fe2–Fe3	61.21(4)	Fe4–Fe3–Fe1	62.19(4)
Fe2–Fe3–Fe1	60.64(5)	Fe2–Fe3–Co1	61.39(4)	Fe3–Fe1–Fe4	60.70(4)
Fe1–C1–C2	167.6(7)	Co1–C2–C1	166.8(5)	Fe4–C1–C2	155.6(7)
C1–C2–Fe	159.4(7)	C2–C1–Fe1	153.9(5)	C1–C2–C3	150.1(9)
—	—	—	—	C2–C3–C4	173.7(8)
—	—	—	—	C3–C4–Fe2	179.0(8)
C1–Fe1–Fe2	49.7(2)	C2–Co1–Fe2	49.6(2)	C1–Fe4–Fe3	50.9(3)
C1–Fe1–Fe3	49.0(2)	C2–Co1–Fe3	50.1(2)	C1–Fe4–Fe1	49.0(3)
Fe2–C1–Fe3	78.5(3)	Fe2–C1–Fe3	67.0(1)	Fe3–C1–Fe1	77.1(3)
Fe2–C2–Fe3	65.3(2)	Fe2–C2–Fe3	77.5(2)	Fe3–C2–Fe1	74.1(2)
C1–Fe2–C2	35.1(2)	C1–Fe2–C2	34.0(2)	C1–Fe3–C2	37.0(3)
C1–Fe3–C2	31.9(2)	C1–Fe3–C2	33.3(2)	C1–Fe1–C2	37.4(3)
Fe1–C11–O11	159.5(9)	Fe3–C33–O33	171(1)	Fe1–C11–O11	157.8(8)
Fe3–C11–O11	122.9(8)	Fe–C–O	175.2–178.8(9)	Fe3–C11–O11	126.0(7)
Fe2–C23–O23	170(1)	Co–C–O	175.1–179.8(9)	Fe–C–O[b]	176.6–179.3(9)
Fe–C–O[b]	176–179(1)	—	—	—	—

[a] O50···O50*: 2.92(2). [b] Parameters for the remaining carbonyl ligands.

The inconsistency between the solid state structure and the very broad ^{1}H-NMR signals observed at r.t. suggested occurrence of a dynamic process in a solution, which was further analyzed by variable temperature ^{13}C-NMR spectra (Fig. 3). The spectrum observed at 25°C containing only one set of the alkyl substituent signals of the C_5Me_4Et ring and a broad CO signal also suggested a dynamic behavior. However, upon cooling to −80°C, a spectrum consistent with the solid state structure was obtained. Two sets of the alkyl and ring carbon signals of the C_5Me_4Et ligands were observed in higher field, corresponding to the two C_5Me_4Et rings in the cluster core and the isolated Fe(η^5-C_5Me_4Et)$(CO)_2$ group. The C1 and C2 signals were located at δ_C 153.5 and 207.8, which were comparable to the chemical shift values of the corresponding acetylide carbon signals of the related tetranuclear dicarbide complex (η^5-C_5Me_5)$FeCo_2(CO)_6$(μ_3-η^1:η^2:η^2-C≡C–Fe(η^5-C_5Me_5)$(CO)_2$) **6** [obtained from **2** and $Co_2(CO)_8$ ([6]e)] and trinuclear μ_3-η^1:η^2:η^2-acetylide cluster compounds [8]. As for the CO signals, those involved in the Fe(η^5-C_5Me_4Et)$(CO)_2$ moiety appeared as a sharp resonance and the terminal CO ligands attached to the Fe_3 core were observed as a broad signal owing to the rotational process of the $Fe(CO)_3$ units still operating at this temperature. The semi-bridging CO ligand was located at δ_C 231.2 as was consistent with the results of the X-ray and IR studies and, therefore, the unsymmetrical structure was found to be retained in a solution at a lower temperature. At −40°C, the most and the second most deshielded signals coalesced into the single broad signal indicating all CO ligands attached to the Fe_3 core scrambled. Above −10°C the CO signal of the distal Fe(η^5-C_5Me_4Et)$(CO)_2$ group and the cluster CO signals coalesced into the single resonance, and the C_2 signals and C_5Me_4Et ring carbon signals disap-

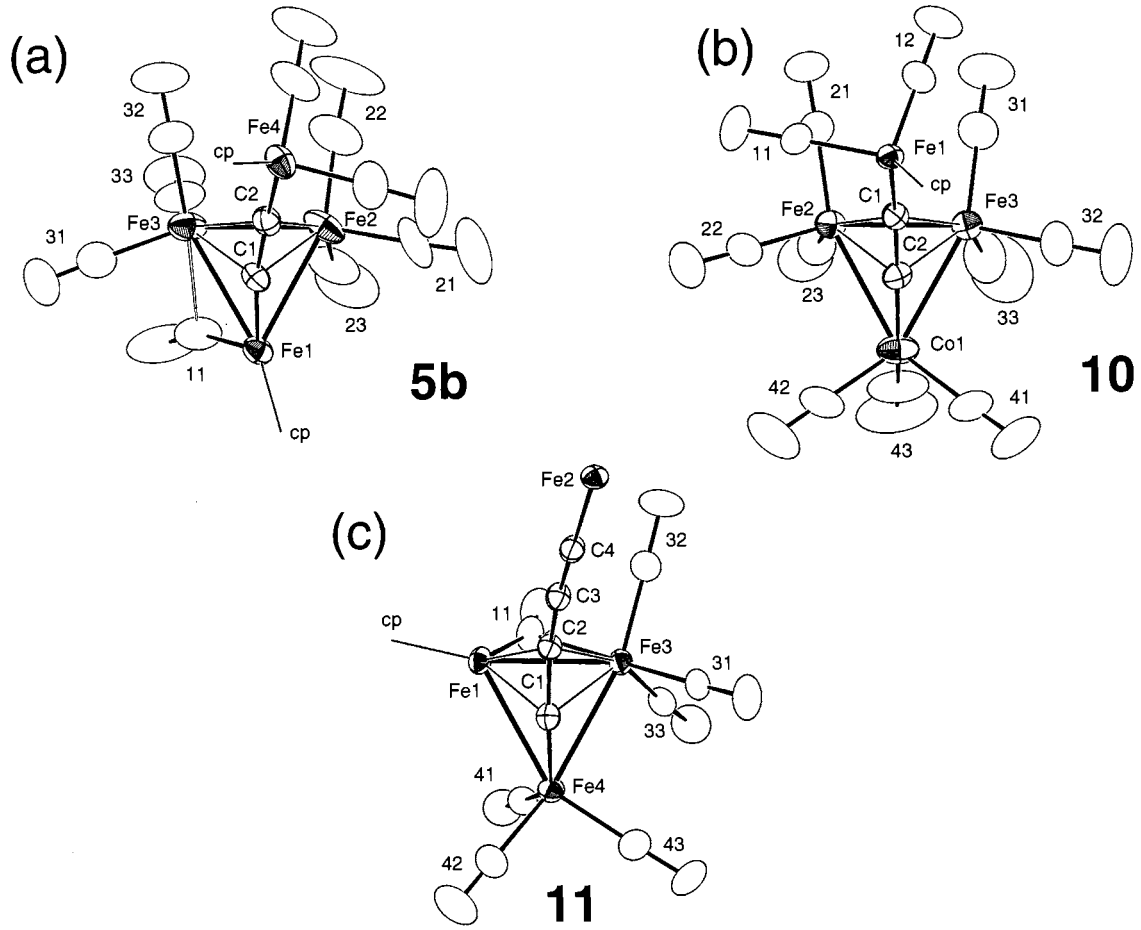

Fig. 2. Core structures of the tetrairon acetylide cluster compounds. Labels without atom names are for the CO ligands. (a) **5b**. (b) **10**. (c) **11**.

peared. The variable temperature ^{13}C-NMR experiment revealed that, at a higher temperature, the two C_5Me_4Et groups and the two C_2 carbon atoms became equivalent and all the CO ligands coalesced into a single resonance, although attempts to obtain a spectrum at a fast exchange limit were unsuccessful due to thermal decomposition at higher temperatures. Similar dynamic behavior was already reported for the $Fe_2Co_2(\mu_4\text{-}C_2)$ cluster compound **6** by us ([6]e).

The fact that the two C_5R_5 groups become equivalent at a higher temperature indicates that a process, whereby the $(\eta^5\text{-}C_5R_5)$Fe unit in the Fe_3 core is kicked out and the $(\eta^5\text{-}C_5Me_4Et)$Fe unit in the distal $Fe(\eta^5\text{-}C_5R_5)(CO)_2$ group is incorporated into the Fe_3 core (Eq. 1), operates at a rate faster than the NMR time scale. Two plausible mechanisms are shown in Scheme 1. One mechanism (i) is an associative one. The isolated $Fe(\eta^5\text{-}C_5R_5)(CO)_2$ group interacts with the Fe_3 core to form a symmetrical intermediate **7** with a butterfly structure. Extrusion of the other $Fe(\eta^5\text{-}C_5R_5)(CO)_2$ group which is originally involved in the cluster core regenerates the equivalent structure **5′**. The other dissociative mechanism (ii) involves initial elimination of the $Fe(\eta^5\text{-}C_5R_5)(CO)_2$ group to give the coordinatively unsaturated species **8** and subsequent coordination of the $Fe(\eta^5\text{-}C_5R_5)(CO)_2$ group of the other side also furnishes **5′**. The coalescence of all the CO signals can be interpreted in terms of CO-scrambling at the stage of **5** or **7**. If these processes occur at a rate faster than the NMR time scale, the above-mentioned phenomena will be observed. The MO calculation for the Ru_4 analogue of **5** by Halet et al. ([2]a) predicts that the coordinatively unsaturated intermediate corresponding to **8** is more stable than the butterfly structure corresponding to **7**. In contrast to the Fe_2Co_2 derivative **6** which does not react with 2e-donors, the Fe_4 cluster **5** slowly reacts with CO and PPh_3 (see below) indicating viability of participation of a coordinatively unsaturated species. Although these results support mechanism (ii), the two mechanisms can not be discriminated by the obtained NMR data alone. In addition, a rotational process of the acetylide moiety on the Fe_3 cluster face may be feasible, because an isomeric structure analogous to the twisted structure **9** is actually observed for the adduct of the butadiynediyl complex (**11**; see below). In this case, too, no definitive conclusion for the occurrence of such process can be obtained by the data available at this moment.

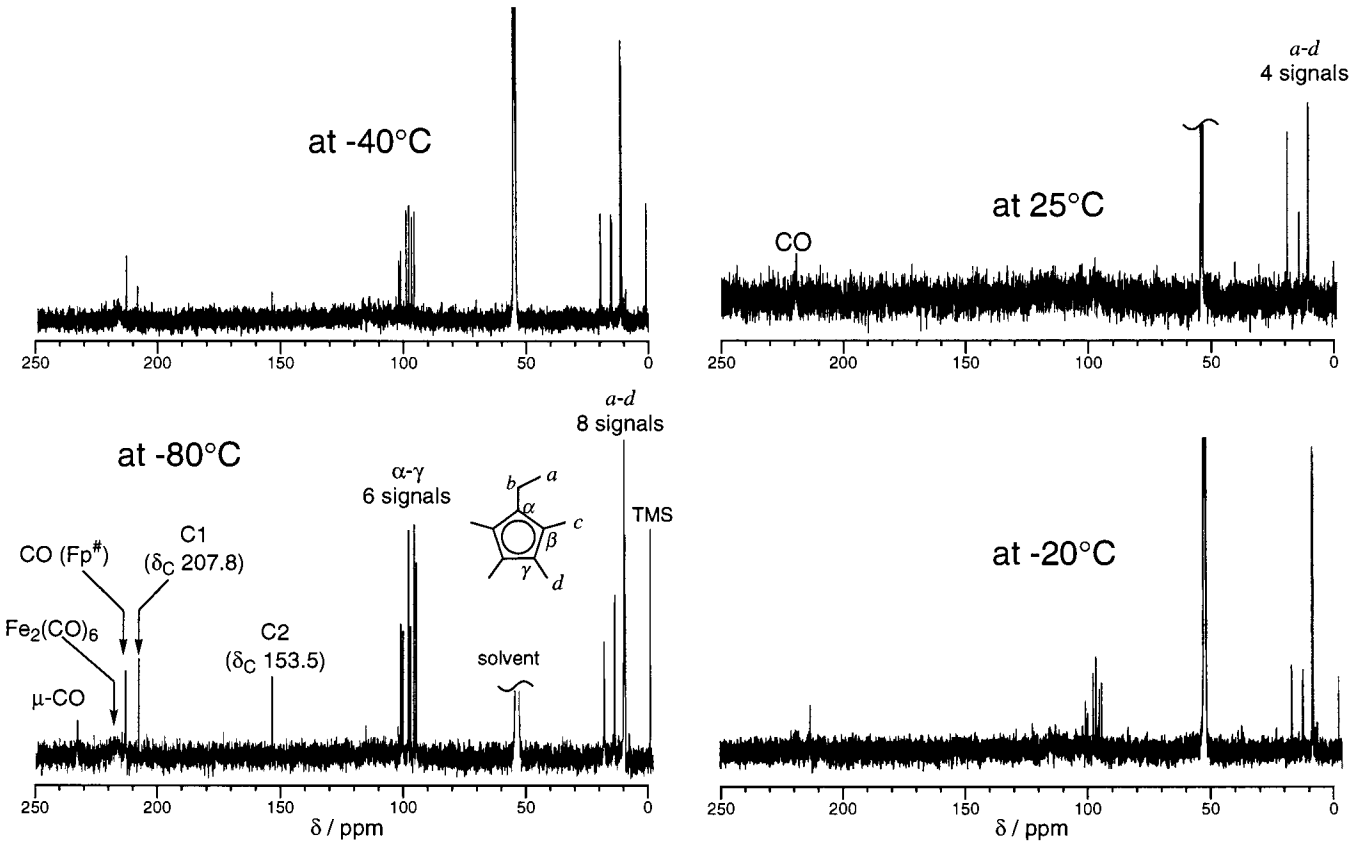

Fig. 3. Variable temperature ^{13}C-NMR spectra of **5b** (observed at 100 MHz in CD_2Cl_2).

Although a number of fluxional transition metal cluster compounds have been reported so far [9], most of them are based on moving of ligands among the transition metal centers. The present system belongs to a rare class of compounds which show dynamic behavior by way of reversible metal–metal bond scission and recombination processes ([6]e).

Some reactivities of **5b** were examined, though they were not so remarkable. The dicarbide complex **5b** was found to react with 2e-donors such as PPh_3 and CO [10]. Despite many attempts of isolation, pure products were not obtained, although formation of a considerable amount of $[Fe(\eta^5\text{-}C_5Me_4Et)(CO)_2]_2$ was evident. Cluster structure expansion was attempted by treatment with polynuclear metal carbonyl species. Although reaction with $Ru_3(CO)_{12}$ gave a mixture of unidentified products, reaction with $Co_2(CO)_8$ resulted in replacement of a metal fragment rather than expected cluster core expansion as revealed by X-ray crystallography (, Fig. 4 and Table 1). In the resultant Fe_3Co mixed metal cluster compound **10**, the $(\eta^5\text{-}C_5Me_4Et)Fe(CO)$ moiety in **5b** was replaced by the isolobal $Co(CO)_3$ fragment and the coordination of the acetylide ligand $[\mu_3\text{-}\eta^1\text{:}\eta^2\text{-}C{\equiv}C\text{–}Fe(\eta^5\text{-}C_5Me_4Et)(CO)_2]$ to the Fe_2Co triangle was found to be symmetrical as indicated by the similar Fe2–C2 [1.990(5) Å] and Fe3–C2 distances [2.002(6) Å]. The difference (0.01 Å) was much smaller than that of the Fe_4 cluster compound **5b** (0.27 Å) (see above). Meanwhile the C≡C length [1.259(7) Å] was comparable to that in **5b** [1.292(9) Å]. Although compounds **10b** and **5b** are isoelectronic with each other, any dynamic process is not observed for **10b** as observed for **5b**.

*2.2. Interaction of butadiynediyl complex **2** with $Fe_2(CO)_9$ leading to acetylide cluster compound **11** and μ_3-η^3-propargylidene–ketene compound **12***

Reaction of **2** with $Fe_2(CO)_9$ afforded two types of

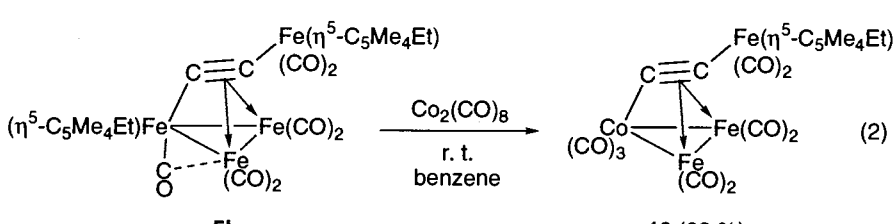

5b **10** (23 %)

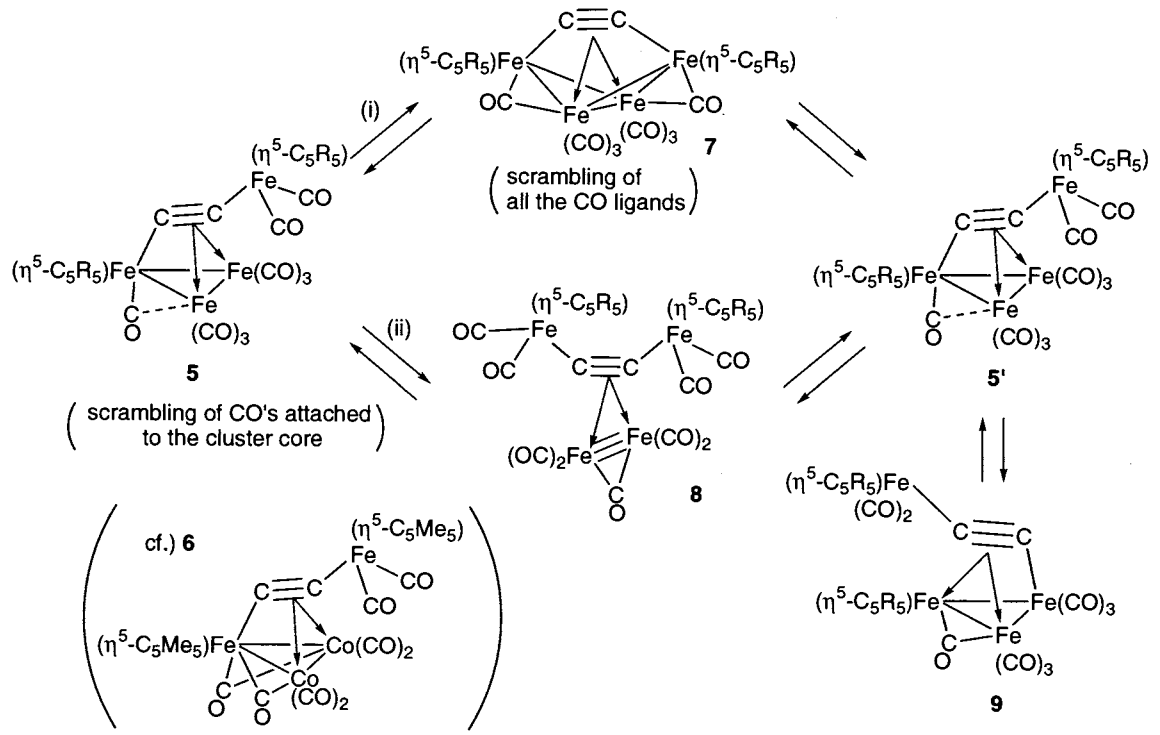

Scheme 1. Two plausible mechanisms showing the (η^5-C_5R_5)Fe unit in the Fe_3 core being kicked out and the (η^5-C_5Me_4Et)Fe unit in the distal Fe(η^5-C_5R_5)$(CO)_2$ group being incorporated into the Fe_3 core by (i) an associative and (ii) a dissociative route.

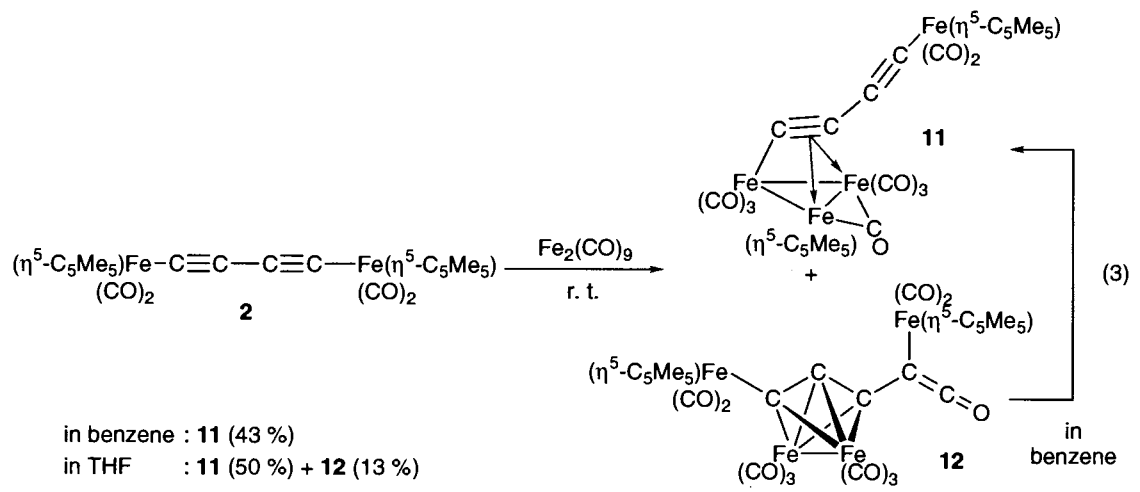

tetrairon adducts **11** and **12** depending on the reaction conditions. The reaction in benzene gave the acetylide cluster-type nonacarbonyl compound **11** exclusively, whereas the reaction in THF produced a small amount of the decacarbonyl ketene compound **12** in addition to **11**. It is notable that **12** was not formed in benzene and dissolution of an isolated sample of **12** in benzene resulted in the conversion to **11** after 44 h. Attempted synthesis of a higher nuclearity cluster compound by treatment with an excess amount of $Fe_2(CO)_9$ was unsuccessful probably owing to protection of the unreacted C≡C part by the bulky Fe(η^5-C_5Me_5)$(CO)_2$ group and the cluster moiety.

Both of the tetrairon complexes were characterized by X-ray crystallography (Figs. 5 and 6; Tables 1 and 2). The structure of **11** can be described as a trinuclear μ_3-η^1:η^2:η^2-acetylide [C≡C–C≡C–Fe(η^5-C_5Me_5)$(CO)_2$] cluster compound and the C3≡C4–Fe(η^5-C_5Me_5)$(CO)_2$ part has no interaction with the Fe_3 cluster core. One of the characteristic features of **11** is that the Fe(η^5-C_5Me_5)$(CO)_2$ group originally σ-bonded to the C≡C–C≡C rod in **2** moves to the π-bonded site. Although the structure of the trinuclear (η^5-C_5Me_5)$Fe_3(CO)_7$ core is not symmetrical

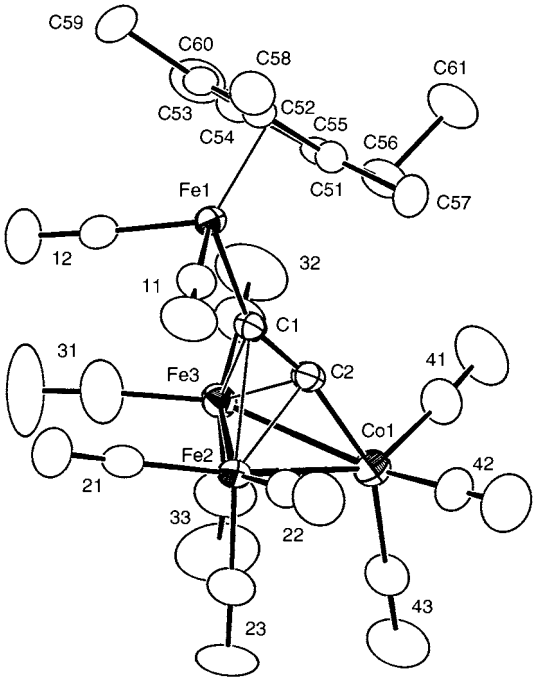

Fig. 4. Molecular structure of **10** drawn at the 30% probability level. Labels without atom names are for the CO ligands.

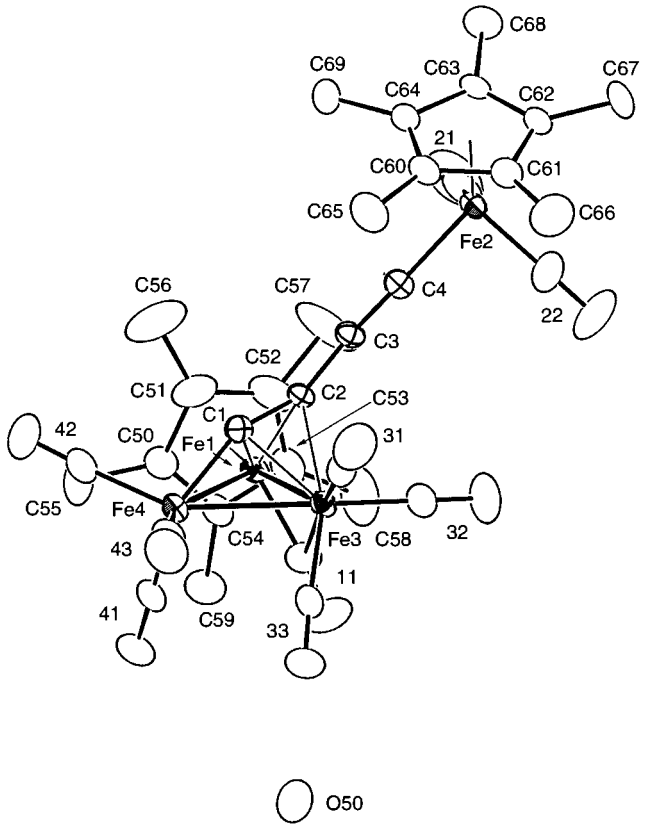

Fig. 5. Molecular structure of **11**·H_2O drawn at the 30% probability level. Labels without atom names are for the CO ligands.

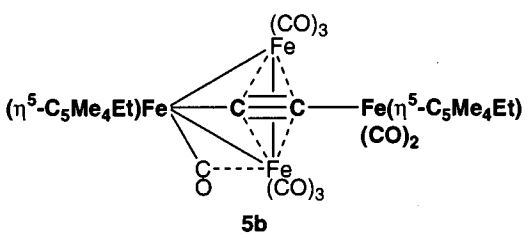

5b

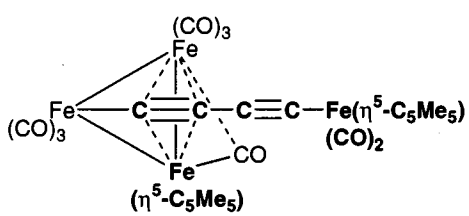

11

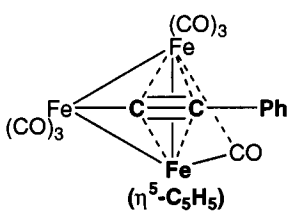

13

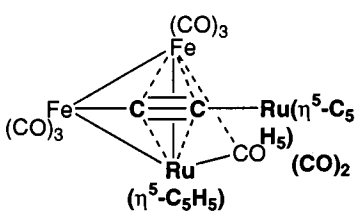

14

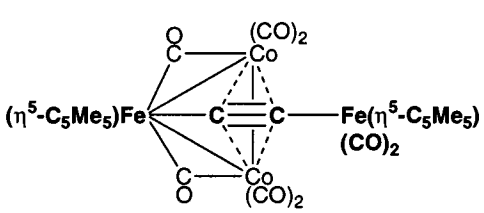

6

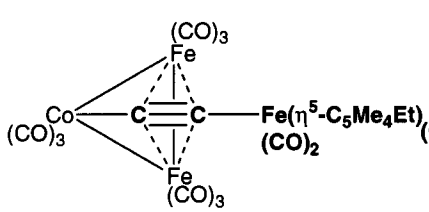

10

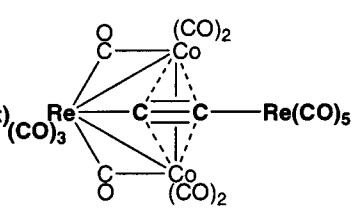

15

Chart 1.

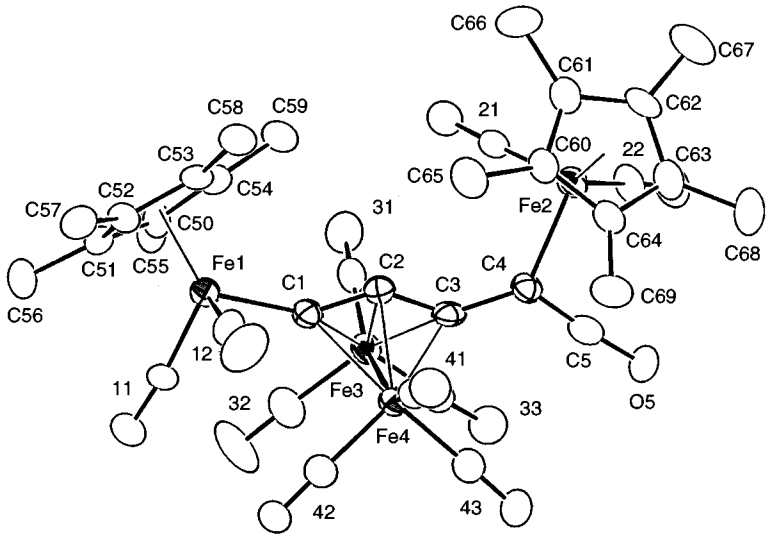

Fig. 6. Molecular structure of **12** drawn at the 30% probability level. Labels without atom names are for the CO ligands.

with respect to the plane passing through the Fe–C≡C–C≡C–Fe(η^5-C_5Me_5)$(CO)_2$ linkage, the π-coordinations are found to be rather symmetrical as indicated by the Fe1–C2 [2.080(7) Å] and Fe3–C2 distances [2.096(7) Å] with the small difference < 0.02 Å.

Similar coordination site change ($\sigma \rightarrow \pi$) has been noted for related acetylide cluster compounds (Chart 1; The original acetylide linkages are bold-faced). In 1975 Yamazaki et al. reported formation of the triiron acetylide cluster compound **13** by interaction of the phenylacetylide complex Fe(η^5-C_5H_5)$(CO)_2$–C≡C–Ph with $Fe_2(CO)_9$ and it was found that the Fe(η^5-C_5H_5) group was π-coordinated to the acetylide part [11]. Meanwhile, dicarbide cluster compounds have been synthesized by addition of dimetallic species to ethynediyl complexes as reported by us (**6**) ([6]e), Selegue (**14**) [12] and Beck (**15**) [13] (Chart 1). Several conclusions can be deduced from their comparison. In the series of (η^5-C_5R_5)$M_3(CO)_7$(μ-C≡C–X)-type complexes (M: Group 8 elements (Fe, Ru); **5b**, **11**, **13** and **14**), the (η^5-C_5R_5)$Fe_3(CO)_7$ core structures are unsymmetrical with respect to the C≡C–X part. In sterically congested η^5-cyclopentadienyl transition metal carbonyl complexes, carbonyl ligands often interact with an adjacent metal center in a semibridging fashion as found for **5b** [14]. This interaction causes an unsymmetrical structure, which gives rise to an opportunity of formation of another unsymmetrical structure (twisted structure) where the M(η^5-C_5R_5) unit occupies the π-coordinated site as found for **11**, **13** and **14** [15]. When the electron-donating abilities of the Fe(η^5-C_5R_5)(CO) and $Fe(CO)_3$ fragments are compared, the former is more electron-donating than the latter and, therefore, effective back-donation from the Fe(η^5-C_5R_5) part to the π*-orbitals of the C≡C moiety would stabilize the twisted structure rather than the symmetrical structure. In particular, replacement of the Fe(η^5-C_5Me_4Et) part in **5b** by the more-electron-donating Ru(η^5-C_5H_5) unit (**14**) apparently causes structural isomerization, although the Fe_4 and the Fe_2Ru_2 complexes are isoelectronic compounds. In contrast, in the case of complexes **6**, **10** and **15** which lack a C_5R_5 ligand in the metal-triangle, there is no

Table 2
Selected structural parameters for **12**

Bond lengths (Å)			
Fe–C1	1.95(1)	Fe4–C1	2.22(1)
C1–C2	1.33(1)	Fe4–C2	2.06(1)
C2–C3	1.34(1)	Fe4–C3	2.02(1)
C3–C4	1.45(1)	Fe3–Fe4	2.484(2)
C4–Fe2	2.05(1)	Fe–CO	1.72–1.80(1)
C4–C5	1.32(1)	C–O	1.13–1.19(1)
C5–O5	1.21(1)	Fe–C(C_5Me_5)	2.09–2.16(1)
Fe3–C1	2.18(1)	C–C(C_5Me_5)	1.40–1.46(1)
Fe3–C2	2.05(1)	C–Me(C_5Me_5)	1.45–1.54(2)
Fe3–C3	2.10(1)		
Bond angles (°)			
Fe1–C1–C2	146.3(9)	C3–Fe4–Fe3	54.3(3)
C1–C2–C3	141(1)	C1–Fe3–C2	36.6(4)
C2–C3–C4	141(1)	C2–Fe3–C3	37.8(4)
C3–C4–Fe2	130.8(8)	C1–Fe4–C2	36.1(4)
Fe3–C1–Fe4	68.8(3)	C2–Fe4–C3	38.4(4)
Fe3–C2–Fe4	74.5(4)	C3–C4–C5	125(1)
Fe3–C3–Fe4	74.2(4)	Fe2–C4–C5	104.0(8)
C1–Fe3–Fe4	56.3(3)	C4–C5–O5	174(1)
C2–Fe3–Fe4	52.9(3)	Fe–C–O	173–179(1)
C3–Fe3–Fe4	51.6(3)	C–C–C(C_5Me_5)	106–110(1)
C1–Fe4–Fe3	54.9(3)	C–C–Me(C_5Me_5)	122–130(1)
C2–Fe4–Fe3	52.6(3)		

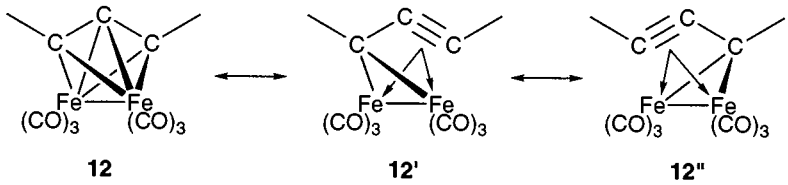

Scheme 2. The two canonical μ-η^3:η^3-propargylidene structures **12**′ and **12**″.

chance for a semi-bridging CO interaction leading to an unsymmetrical structure.

At this moment, we can not draw any conclusion about the addition mechanism of the $Fe_2(CO)_m$ unit to the acetylide complex. Also we have no idea if the twisted structure arises from isomerization (twisting over the M_3 face) of the symmetrical form. Selegue et al. proposed a stepwise double addition mechanism of mononuclear $Fe(CO)_n$ species to interpret the formation of the unsymmetrical complex **14** [12]. However, because the addition reaction of $Fe_2(CO)_9$ to acetylide complexes has been found to be rather selective compared to that to organic acetylenes and, furthermore, products arising from addition of more than three $Fe(CO)_n$ units have not been isolated from the reactions of acetylide complexes, a mechanism involving addition of a dimetallic species $Fe_2(CO)_m$ may not be excluded.

The unique structure of the other product **12** contains the ketene functional group in addition to the diiron μ-η^3:η^3-propargylidene structure [16]. Although spectroscopic identification of the ketene part is obscured owing to overlap of their characteristic IR and ^{13}C-NMR absorptions with those of the CO ligands, the structural parameters clearly indicates the presence of a ketene functional group. The C1–C2–C3 part in **12** interacts with both of the diiron center in η^3-fashion and, judging from the similar C1–C2 (1.33(1) Å) and C2–C3 distances (1.34(1) Å), the coordinatively saturated trigonal-bipyramidal Fe_2C_3 core can be described as a resonance hybrid of the two canonical μ-η^3:η^3-propargylidene structures **12**′ and **12**″ (Scheme 2). The ^{13}C-NMR signals of the carbon atoms in the propargylidene structure are located at 110.4, 114.3 and 160.7 ppm. To our knowledge, no precedented report on such a coordination structure has appeared ([3]v).

Plausible formation mechanisms of **11** and **12** are shown in Scheme 3, although other mechanisms such as one involving stepwise addition processes of mononuclear species are also possible. Initial coordination of one of the two C≡C bonds in **2** gives the ($\perp$)-μ-η^2:η^2-intermediate **16**. Two pathways are feasible hereafter. Interaction of the proximal Fe(η^5-C_5Me_5)$(CO)_2$ group with the diiron part (path *a*) furnishes the acetylide cluster **11** after decarbonylation. In the meantime, the approach of the C≡C bond on the other side may form a η^4-intermediate **17** (path b), though the ($\perp$)-form **17a** may be highly strained. Subsequent CO insertion and metal–metal bond formation associated with decarbonylation furnish the ketene compound **12**. The conversion of **12** into **11** should be initiated by decarbonylation from the $Fe_2(CO)_6$ moiety. Final associative interaction of the proximal Fe(η^5-C_5Me_5)$(CO)_2$ group coupled with the C–CO bond cleavage furnishes **11**. It has been reported that the C=C bond in ketene can be cleaved within the coordination sphere of a transition metal species [16]. Thus **11** can be formed either by the direct reaction of **2** with $Fe_2(CO)_9$ or decarbonylation of the decacarbonyl ketene compound **12**.

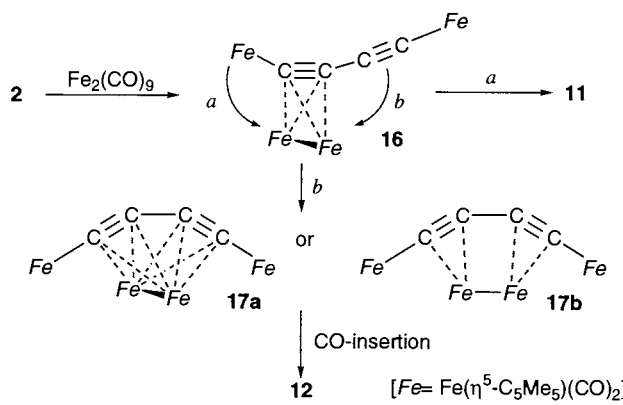

Scheme 3. Plausible formation mechanisms for complexes **11** and **12**.

*2.3. Interaction of ethynyl complex **3** with $Fe_2(CO)_9$: formation of quinone **18** and acetylide cluster compound **19***

In contrast to the reactions of the ynediyl complexes mentioned above, the reaction of polyynyl complexes is complicated as found for the reactions of organic acetylene molecules [7]. Treatment of the ethynyl complex **3a** with $Fe_2(CO)_9$ in benzene at r.t. afforded a mixture of products.). Of the three isolated products, the orange (**18a**) and purple ones (**19**) were characterized successfully, though the green one decomposed during purification processes.

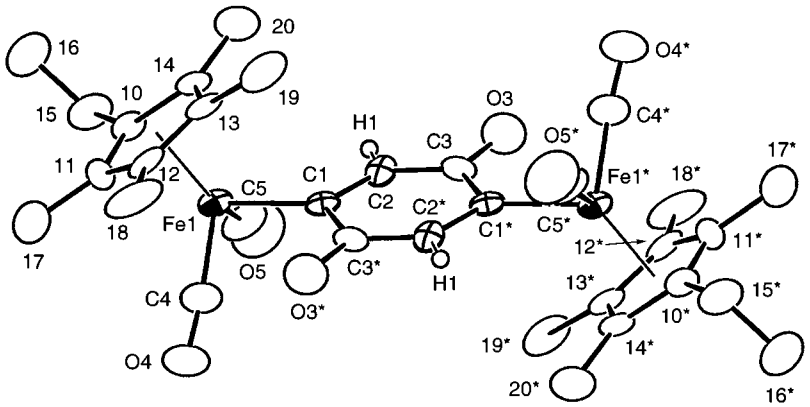

Fig. 7. Molecular structure of **18b** drawn at the 30% probability level. Labels without atom names are for the carbon atoms of the C_5Me_5 ligands.

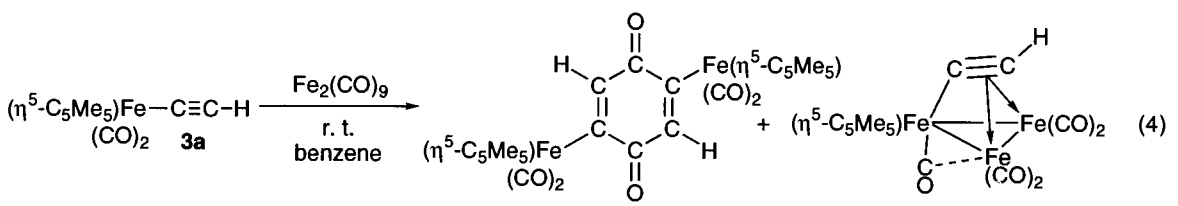

orange **18a** (15 %) *purple* **19** (15 %)

Both of the products show quite simple spectral patterns. For example, ^{1}H-NMR spectra contain two singlet signals in a 1:15 ratio suggesting that C_5Me_5 and C_2H units were incorporated in a 1:1 ratio. The orange product **18a** has been characterized as a quinone complex on the basis of the X-ray crystallographic result of the Fe(η^5-C_5Me_4Et)$(CO)_2$ derivative **18b** (Fig. 7 and Table 3). In accord with the structure, an IR spectrum of **18b** contains a ν(C=O) band at 1616 cm^{-1} in addition to the two ν(C≡O) vibrations due to the Fe(η^5-C_5Me_4Et)$(CO)_2$ part. When the molecular structure is inspected in detail (Scheme 4), the C1–C2 and C3–O3 distances are longer than the normal C(sp^2)=C(sp^2) (1.34 Å) and C(sp^2)=O(sp^2) distances (1.20 Å) and, by contrast, C2–C3 distance [1.45(2) Å] is shorter than the normal C(sp^2)–C(sp^2) distances (1.48 Å). These deformations should arise from contribution of the zwitterionic structure **18b′**. Accordingly, the slightly shorter Fe–C1 length and the deshielding of the δ_C(C1) signal (188.1 ppm; cf. δ_C(=CH) 154.7) support the carbene character of the Fe–C1 moiety and π-back-donation to the quinone ring was evidenced by the red shift of the ν(C=O) vibration by ca. 60 cm^{-1} compared to quinones with organic substituents.

The purple product **19** has been characterized as a triiron acetylide cluster compound by comparison of its spectral data with those of the tetrairon complex **5b**. The doublet ^{13}C-NMR signals of the C_2H part are located at δ_C 117.2 (d, ^1J = 222 Hz) and 198.0 (d, ^2J = 9 Hz), which are close to the corresponding signals of **5b** (see above), and the very large $^1J_{CH}$ coupling constant suggests that the C_2H part is an acetylide ligand. The molecular weight estimated by an FD-MS spectrum

Table 3
Selected structural parameters for **18b**

Bond lengths (Å)			
Fe–C1	1.94(1)	Fe1–C5	1.87(2)
C1–C2	1.37(2)	C4–O4	1.17(2)
C1–C3*	1.52(2)	C5–O5	1.08(2)
C2–C3	1.45(2)	Fe–C(C_5Me_5)	2.10–2.15(1)
C3–O3	1.24(1)	C–C(C_5Me_5)	1.39–1.48(2)
Fe1–C4	1.74(1)	C–Me(C_5Me_5)	1.45–1.51(2)
Bond angles (°)			
Fe1–C1–C2	127(1)	C2–C3–O3	116(2)
Fe1–C1–C3*	122(1)	C1*–C3–O3	119(1)
C2–C1–C3*	111(1)	Fe1–C4–O4	175(2)
Fe1–C2–C3*	122(1)	Fe1–C5–O5	177(2)
C1–C2–C3	125(1)	C–C–C(C_5Me_5)	104–112(1)
C2–C3–C1*	124(1)	C–C–Me	122–131(2)

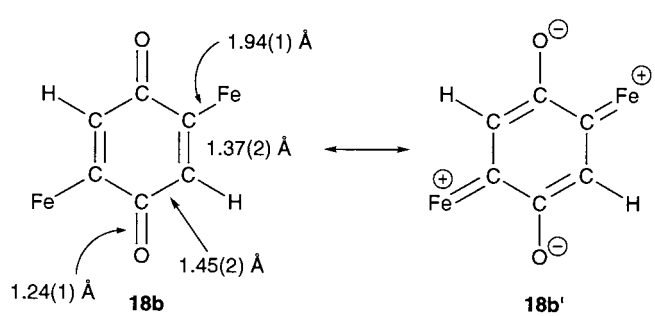

Scheme 4. Interconversion of complexes **18b** and **18b′**.

($m/z = 524$) indicates that the composition of **19** is (η^5-C_5Me_5)Fe(μ-C_2H)$(CO)_7$. In addition, the ν(CO) band in the lower energy region (1851 cm^{-1}) similar to that in **5** suggests the presence of a semi-bridging CO ligand. These spectral features are consistent with the structure depicted in Eq. 4 (the μ-C≡C–H derivative of **5**), although the possibility of the isomeric twisted structure as discussed above can not be eliminated.

The trinuclear cluster compound **19** may be formed by decarbonylation of an adduct of **3** to an Fe_2 species, [μ-(η^5-C_5R_5)$(CO)_2$Fe–C≡C–H]$Fe_2(CO)_n$. The quinone complex **18** is a formal 2:2 adduct of **3** and CO. Similar catalytic and stoichiometric synthesis of quinones from acetylene and CO is reported, though definitive mechanisms have not been established [17].

We also examined reaction of the butadiynyl complex **4** with $Fe_2(CO)_9$. Although the reaction appeared to be cleaner than that of the ethynyl complex **3**, the products decomposed during TLC separation.

3. Conclusions

Interaction of the ethynediyl diiron complex **1** with $Fe_2(CO)_9$ results in selective formation of the tetrairon C_2 complex **5**, which exhibits the dynamic behavior via reversible Fe–Fe bond scission and recombination processes as analyzed by variable temperature ^{13}C-NMR.

The reaction of the butadiynediyl complex **2** also produced the acetylide cluster-type tetraironnonacarbonyl compound **11**. Although the composition and the trinuclear acetylide cluster-type structure of **11**, (μ_4-C_4)Fe_4(η^5-C_5R_5)$_2(CO)_9$, is quite similar to those of **5**, (μ_4-C_2)Fe_4(η^5-C_5R_5)$_2(CO)_9$, the C_4 complex **11** does not show dynamic behavior via Fe–Fe bond scission due to the isolated Fe(η^5-C_5R_5)$(CO)_2$ group being not within the distance of interaction with the triiron cluster part. The second reaction product from **2** is the decacarbonyl complex **12**, which contains two unique structures: the μ_3-η^3-propargylidene and ketene functional groups. The two tetrairon complexes can be interconverted via addition and removal of carbonyl ligands.

Although selective reaction has not been observed for the ethynyl (**3**) and butadiynyl complexes (**4**), the reaction of **3** affords the unique dimetalated quinone **18** which contains the electron-releasing and -withdrawing parts in a molecule.

Combined with the present result, structure expansion of **1**–**4** by the action of other metal species, which is now under study, would establish a network of polynuclear C_4 species analogous to that of polynuclear C_2 species [2,6].

4. Experimental section

4.1. General methods

All manipulations were carried out under an inert atmosphere by using standard Schlenk tube techniques. Ether and hexanes (Na–K alloy) and CH_2Cl_2 (P_2O_5) were treated with appropriate drying agents, distilled, and stored under argon. The iron complexes **1**–**4** ([6]b,p) and $Fe_2(CO)_9$ [18] were prepared according to the published procedures. Other chemicals were purchased and used as received. Column chromatography was performed on alumina [aluminum oxide, activity II–IV (Merck Art. 1097); preparative TLC: aluminum oxide 60 PF_{254} (Typ E) (Merck Art. 1103)]. ^{1}H- and ^{13}C-NMR spectra were recorded on a JEOL EX400 (^{1}H: 400 MHz; ^{13}C: 100 MHz) spectrometer. Solvents for NMR measurements containing 0.5% TMS were dried over molecular sieves, degassed, distilled under reduced pressure, and stored under Ar. IR and FD-MS spectra were obtained on a JASCO FT/IR 5300 spectrometer and a Hitachi M80 mass spectrometer, respectively.

4.2. Interaction of *1a* with $Fe_2(CO)_9$

A mixture of **1a** (400 mg, 0.77 mmol) and $Fe_2(CO)_9$ (840 mg, 2.31 mmol) dissolved in benzene (25 ml) was stirred overnight at ambient temperature. After removal of the volatile under reduced pressure, the residue was extracted with THF and passed through a Celite pad. The filtrate was concentrated to 1–2 ml and hexane was added. The resulting suspension was poured onto the top of an alumina column and was eluted with THF:hexanes ratio 1:8. After small amounts of Fe(η^5-C_5Me_5)$(CO)_2$ and **1a** were eluted, the product was collected by elution with THF. Removal of the volatiles and crystallization from CH_2Cl_2–hexanes gave **5a** as black microcrystals (0.294 mmol, 0.38 mmol, 50% yield). Because the resulting crystalline material was virtually insoluble in organic solvents, analyses were performed for the C_5Me_4Et derivative **5b**. **5a**: IR (KBr) 2039, 2018, 2002, 1966, 1950, 1900, 1873, 1851 cm^{-1}. Anal. Calc. for $C_{31}H_{30}O_9Fe_4$: C, 48.37; H, 3.90%. Found: C, 48.00; H, 3.70%.

4.3. Interaction of *1b* with $Fe_2(CO)_9$ giving *5b*

A mixture of **1b** (403 mg, 0.74 mmol) and $Fe_2(CO)_9$ (808 mg, 2.22 mmol) dissolved in benzene (25 ml) was stirred overnight at ambient temperature. Work-up as described for **5a** gave **5b** (339 mg, 0.42 mmol, 57% yield) after recrystallization from acetone. **5b**: ^{1}H-NMR (CD_2Cl_2) (at 25°C): δ 1.06 (6H, br, CH_2CH_3), 1.83 (24H, br, C_5Me_4Et), 2.27, 2.40 (2H × 2, br,

CH_2CH_3); (at −80°C) δ 0.92, 1.03 (3H × 2, br, CH_2CH_3), 1.72, 1.92 (12H × 2, br, C_5Me_4Et), 2.10, 2.30 (2H × 2, br, CH_2CH_3). ^{13}C-NMR (in CD_2Cl_2 at −80°C): δ 9.5, 9.6, 9.9, 10.0 (q × 4, J = 128 Hz, C_5Me_4Et), 13.8, 13.9 (q × 2, J = 128 Hz, CH_2CH_3), 17.9, 18.0 (t × 2, J = 156 Hz, CH_2CH_3), 95.0, 96.0, 97.2, 98.2, 100.5, 101.0 (s, C_5Me_4Et), 153.4 (s, Fe(h^5-C_5Me_4Et)$(CO)_2$–C≡), 207.8 (s, Fe(η^5-C_5Me_4Et)$(CO)_2$–C≡C), 213.1 (s, CO in Fe(η^5-C_5Me_4Et)$(CO)_2$), ~218 (br, Fe–CO), 233.0 (s, semi-bridging CO). IR (KBr): 2036, 1994, 1966, 1950, 1904, 1880, 1855 cm^{-1}. Anal. Calc. for $C_{33}H_{34}O_9Fe_4$: C, 49.68; H, 4.26%. Found: C, 49.42; H, 3.94%.

4.4. Reaction of **5b** with $Co_2(CO)_8$ giving **10**

A benzene solution (10 ml) of **5b** (250 mg, 0.30 mmol) and $Co_2(CO)_8$ (307 mg, 0.9 mmol) was stirred for 6 h at ambient temperature. After removal of the volatiles products were extracted with CH_2Cl_2 and passed through an alumina plug. Concentration, addition of haxanes and cooling at −20°C gave **10** (49 mg, 0.069 mmol, 23% yield) as black crystals. **10**: ^{1}H-NMR (C_6D_6): δ 0.61 (3H, t, J = 7.6 Hz, CH_3CH_2), 1.33 (12H, brs, C_5Me_4Et), 1.84 (2H, q, J = 7.6 Hz, CH_2CH_3). ^{13}C-NMR (C_6D_6): δ 8.6, 8.8, 14.2 (q × 3, J = 128 Hz, $C_5Me_4CH_2CH_3$), 18.4 (t, J = 156 Hz, CH_2), 98.0, 99.1, 102.5 (C_5Me_4Et), 212.2, 213.4 (Fe–CO) (the C_2 signals could not be located). IR (KBr): 2077, 2021, 2004, 1984, 1942 cm^{-1}. Anal. Calc. for $C_{22}H_{17}O_9Fe_3Co$: C, 40.54; H, 2.63%. Found. C, 40.42; H, 2.60%.

4.5. Interaction of **2** with $Fe_2(CO)_9$ in benzene giving acetylide cluster compound **11**

A benzene solution (30 ml) of **2** (160 mg, 0.295 mmol) and $Fe_2(CO)_9$ (537 mg, 1.48 mmol) was stirred for 43 h at ambient temperature. After removal of the volatiles, the residue was extracted with CH_2Cl_2 and passed through an alumina plug. Concentration and addition of hexanes followed by cooling to −120°C gave **11** (100 mg, 0.126 mmol, 43% yield) as gray–yellow crystals. From the mother liquor Fe(η^5-C_5Me_5)$(CO)_2$ (13 mg, 0.03 mmol, 12% yield) was isolated after concentration and cooling. **11**: ^{1}H-NMR ($CDCl_3$): δ 1.74, 1.90 (15H × 2, s × 2, $(C_5Me_5)_2$). ^{13}C-NMR ($CDCl_3$): δ 9.6, 10.0 (C_5Me_5), 96.8, 97.8 (C_5Me_5), 105.9, 116.4 (C3, C4), 132.4 (C2), 190.5 (C1), 212.3, 213.7 (Fe–CO), 235.6 (μ-CO). IR (KBr): 2048, 2005, 1977, 1945, 1919, 1835 cm^{-1}. FD-MS: 794 (M^+). Anal. Calc. for $C_{33}H_{32}O_{10}Fe_3$ (**11** + H_2O): C, 48.77; H, 3.94%. Found. C, 48.67; H, 3.74%.

4.6. Interaction of **2** with $Fe_2(CO)_9$ in THF giving **11** and ketene compound **12**

A mixture of **2** (180 mg, 0.33 mmol) and $Fe_2(CO)_9$ (636 mg, 1.75 mmol) was stirred in THF (35 ml) for 17 h at r.t. After the consumption of **2** was checked by TLC, the volatiles were removed under reduced pressure. The resulting residue was extracted with CH_2Cl_2 and passed through an alumina pad. Addition of hexanes and cooling at −20°C gave **12** (38 mg, 0.044 mmol, 13% yield) as yellow crystals. Subsequent concentration followed by cooling at −20°C gave **11** (132 mg, 0.166 mmol, 50% yield) as gray–yellow crystals. **12**: ^{1}H-NMR ($CDCl_3$): δ 1.84, 1.88 (15H × 2, s × 2, $(C_5Me_5)_2$). ^{13}C-NMR ($CDCl_3$): δ 9.8, 10.0 (C_5Me_5), 42,9 (>C=C=O), 97.4, 99.8 (C_5Me_5), 110.4, 114.3, 160.7 (C_3Fe_2), 213.5, 214.2, 215.9 (Fe–CO), 215.4 (>C=C=O). IR (KBr): 2059, 2033, 2010, 1993, 1967, 1935 cm^{-1}. FD-MS 850 (M^+). Anal. Calc. for $C_{35}H_{20}O_{11}Fe_4$: C, 49.41; H, 3.56%. Found: C, 49.03; H, 3.30%.

4.7. Conversion of **12** into **11**

A benzene solution (10 ml) of **12** (38 mg, 0.044 mmol) was stirred for 44 h at r.t. Removal of the volatiles, extraction of the residue with CH_2Cl_2 and filtration through an alumina pad gave **11** (32 mg, 0.041 mmol, 92% yield) as confirmed by ^{1}H-NMR.

4.8. Interaction of **3a** with $Fe_2(CO)_9$ giving quinone **18a** and triironacetylide cluster compound **19**

A benzene solution (12 ml) of **3a** (399 mg, 1.47 mmol) and $Fe_2(CO)_9$ (640 mg, 1.76 mmol) was stirred for 3 h at ambient temperature. After removal of the volatiles, the residue was extracted with CH_2Cl_2 and passed through a Celite pad. The filtrate was concentrated and subjected to preparative TLC separation. Elution with ether–hexanes (1:3) gave many bands, from which three major bands were collected. From the orange band, the orange quinone complex **18a** (66 mg, 0.11 mmol, 15% yield) was isolated after crystallization from CH_2Cl_2–hexanes. From the purple band, the purple acetylide cluster compound **19** (115 mg, 0.22 mmol, 15%) was isolated after crystallization from ether–hexanes. Attempted crystallization of the minor product from the third green band resulted in color change to amber–brown. **18a**: ^{1}H-NMR ($CDCl_3$): δ 1.73 (30H, s, $(C_5Me_5)_2$), 7.32 (2H, s, =CH). ^{13}C-NMR ($CDCl_3$): δ 9.5 (q, J = 128 Hz, C_5Me_5), 96.3 (s, C_5Me_5), 155.0 (d, J = 160 Hz, =CH), 184.1 (s, Fe–C=), 189.0 (s, >C=O), 216.7 (s, Fe–CO). IR (KBr): 1997, 1954, 1618 cm^{-1}. FD-MS 600 (M^+). An analytically pure sample was not obtained. **19**: ^{1}H-NMR ($CDCl_3$): 1.79 (15H, s, (C_5Me_5)), 7.41 (1H, s, C_2H). ^{13}C-NMR ($CDCl_3$): δ 9.4 (q, J = 128 Hz, C_5Me_5), 95.8 (s, C_5Me_5), 117.2 (s, J = 222 Hz, ≡CH), 198.0 (d, ^2J = 9 Hz, C≡CH), 213.3 (s, Fe–CO), 231.2 (s, semi-bridging CO). FD-MS 524 (M^+). Anal. Calc. for $C_{19}H_{16}O_7Fe_3$: C, 43.57; H, 3.06%. Found: C, 43.59; H, 3.01%.

Table 4
Crystallographic data

Complex	**5b**	**10**	**11**·H_2O	**12**	**18b**
Formula	$C_{33}H_{34}O_9Fe_4$	$C_{24}H_{17}O_{11}Fe_3Co$	$C_{33}H_{32}O_{10}Fe_4$	$C_{35}H_{30}O_{11}Fe_4$	$C_{32}H_{36}O_6Fe_2$
Formula weight	798.0	707.9	812.0	850.0	628.3
T (°C)	25	25	−60	−60	25
Crystal system	Triclinic	Monoclinic	Triclinic	Triclinic	Triclinic
Space group	$P\bar{1}$	$P2_1/c$	$P\bar{1}$	$P\bar{1}$	$P\bar{1}$
a (Å)	16.624(7)	15.099(4)	12.993(2)	11.708(6)	8.268(4)
b (Å)	17.567(7)	12.600(2)	14.427(3)	16.763(3)	13.262(3)
c (Å)	9.960(2)	14.910(3)	9.918(3)	9.835(2)	7.165(3)
α (°)	97.12(3)	—	97.99(2)	96.46(1)	93.80(3)
β (°)	98.36(3)	100.19(2)	94.25(2)	110.97(3)	103.65(4)
γ (°)	140.39(2)	—	76.01(2)	78.70(2)	81.03(3)
V (Å^3)	1701(4)	2791(2)	1781.5(7)	1756(1)	753.7(5)
Z	2	4	2	2	1
$D_{calc.}$ (g cm^{-3})	1.56	1.68	1.51	1.61	1.38
μ (cm^{-1})	17.2	21.7	16.5	16.8	10.0
2θ (°)	5–50	5–50	5–54	5–54	5–55
No. of data collected	6363	5367	6448	5697	3727
No. of data with $I>3\sigma(I)$	3251	3230	5292	3827	1869
No. of variables	415	352	424	451	181
R	0.056	0.043	0.060	0.077	0.115
R_w	0.042	0.035	0.089	0.081	0.103

4.9. Preparation of **18b** (C_5Me_4Et derivative of **18a**)

The C_5Me_4Et derivative (**18b**) for X-ray crystallography was obtained from reaction between **3b** (560 mg, 1.96 mmol) and $Fe_2(CO)_9$ (855 mg, 2.35 mmol) in benzene (24 ml). Work-up as described above gave **18b** (118 mg, 0.20 mmol, 20% yield). **18b**: ^{1}H-NMR ($CDCl_3$): δ 1.02 (6H, t, $J=8$ Hz, CH_2CH_3), 1.73, 1.75 (12H × 2, s × 2, C_5Me_4Et), 2.17 (4H, q, $J=8$ Hz, CH_2CH_3), 7.30 (2H, s, =CH). ^{13}C-NMR ($CDCl_3$): δ 9.3, 9.5 (q, $J=128$ Hz, C_5Me_4Et), 14.2 (q, $J=128$ Hz, CH_2CH_3), 18.0 (t, $J=125$ Hz, CH_2CH_3), 95.7, 96.7, 101.1 (s × 3, C_5Me_4Et), 154.7 (d, $J=162$ Hz, =CH), 183.3 (d, $^2J=13$ Hz, Fe–C=), 188.1 (s, >C=O), 216.7 (s, Fe–CO). IR (KBr): 1996, 1945, 1616 cm^{-1}. Anal. Calc. for $C_{30}H_{32}O_6Fe_2$: C, 61.20; H, 5.73%. Found: C, 61.53; H, 5.93%.

4.10. X-ray crystallography

Suitable single crystals were mounted on glass fibers. Diffraction measurements of **5b** were made on a Rigaku AFC-5S automated four-circle diffractometer and those of **10** and **18b** were made on a Rigaku AFC5R automated four-circle diffractometer by using graphite-monochromated Mo–K_α radiation ($\lambda=$ 0.71059 Å). The unit cells were determined and refined by a least-squares method using 20 independent reflections (2θ ca. 20°). Data were collected with a 2θ-ω scan technique. If $\sigma(F)/F>0.1$, a scan was repeated up to three times and the results were added to the first scan. Three standard reflections were monitored at every 150 measurements. The data processing (data collection) was performed on a FACOM A-70 (**5b**) and microvax II computers (**10** and **18b**). In the reduction of data, Lorentz and polarization corrections were made. Empirical absorption corrections (Ψ scan) were made for **10** (transmission factor: 0.57–1.00) and **18b** (transmission factor: 0.46–1.00). Crystallographic data and the results of refinements are summarized in Table 4.

Diffraction measurements of **11** and **12** were made on a Rigaku RAXIS IV imaging plate area detector with Mo–K_α radiation ($\lambda=0.71069$ Å). Indexing was performed from three oscillation images which were exposed for 4 min. The crystal-to-detector distance was 110 mm. Data collection parameters were as follows: the detector swing angle: 6° (**11**), 7° (**12**); number of oscillation images: 24 (**11**), 20 (**12**); the exposed time: 100 min (**11**), 60 min (**12**). The data collections were carried out at −60°C. Readout was performed with the pixel size of 100 × 100 μm. The data processing was performed on an IRIS Indy computer. No absorption correction was made, because attempted empirical absorption correction did not improve the results.

Structure analysis was performed on an IRIS O2 computer by using the teXsan structure solving program system obtained from Rigaku, Tokyo, Japan. Neutral scattering factors were obtained from the standard source [19]. The function minimized was $\Sigma w(|F_o|-|F_c|)^2$ where $w=[\sigma^2(F_o)]^{-1}=4F_o^2\cdot[\sigma^2(F_o^2)]^{-1}$. The schemes for unweighted and weighed agreement factors were as follows: $R=\Sigma\||F_o|-|F_c|\|/\Sigma|F_o|$; $R_w=[(\Sigma w(\||F_o|-|F_c|\|)^2/\Sigma wF_o^2)]^{1/2}$. The structures were solved by a combination of the direct methods (SAPI91,

MITHRIL87 and SHELXL 87) and Fourier synthesis (DIRDIF). Unless otherwise stated, non-hydrogen atoms were refined with anisotropic thermal parameters, and hydrogen atoms were fixed at the calculated positions (C–H 0.95 Å) and were not refined. The rather high *R* value for **18b** is due to the low quality of the crystal. The maximum Fourier peak in the final difference Fourier map is 1.50 e $Å^{-3}$ at a distance of 1.14 Å from the iron atom.

Acknowledgements

We are grateful to the Ministry of Education, Science, Sports and Culture of the Japanese Government for financial support of this research.

References

[1] (a) W. Beck, B. Niemer, M. Wieser, Angew. Chem. Int. Ed. Engl. 32 (1993) 923. (b) H. Lang, Angew. Chem. Int. Ed. Engl. 33 (1994) 547. (c) U. Bunz, Angew. Chem. Int. Ed. Engl. 35 (1996) 969.

[2] C2 complexes: (a) G. Frapper, J.-F. Halet, Organometallics 14 (1995) 5044. (b) G. Frapper, J.-F. Halet, M.I. Bruce, Organometallics 16 (1997) 2590. (c) J. Silvetre, R. Hoffmann, Helv. Chim. Acta 68 (1985) 1461. (d) See also ref. ([6]a) and references cited therein.

[3] C4 and higher complexes: Ru: (a) M.I. Bruce, P. Hinterding, E.R.T. Tiekink, B.W. Skelton, A.H. White, J. Organomet. Chem. 450 (1993) 209. (b) Y. Sun, N.J. Taylor, A.J. Carty, J. Organomet. Chem. 423 (1992) C43. (c) Y. Sun, N.J. Taylor, A.J. Carty, Organometallics 11 (1992) 4293. **W**: (d) M.I. Bruce, M. Ke, P.J. Low, J. Chem. Soc. Chem. Commun. (1996) 2405. (e) M.I. Bruce, B.W. Skelton, A.H. White, N.N. Zaitseva, J. Chem. Soc. Dalton Trans. (1996) 3151. (f) B.E. Woodworth, P.S. White, J.L. Templeton, J. Am. Chem. Soc. 119 (1997) 828. **Fe**: (g) P.J.Kim, M. Masai, K. Sonogashira, N. Hagihara, Inorg. Nucl. Chem. Lett. 6 (1970) 181. (h) A. Wong, P.C.W. Kang, C.D. Tagge, D.R. Leon, Organometallics 9 (1990) 1992. (i) R. Crescenzi, C. Lo Sterzo, Organometallics 11 (1992) 4301. (j) N. Le Narvor, C. Lapinte, J. Chem. Soc. Chem. Commun. (1993) 357. (k) N. Le Narvor, L. Toupet, C. Lapinte, J. Am. Chem. Soc. 117 (1995) 7129. (l) F. Coat, C. Lapinte, Organometallics 15 (1996) 477. **Re**: (m) J.A. Ramsden, A. Arif, J.A. Gladysz, J. Am. Chem. Soc. 114 (1992) 6809. (n) J.A. Ramsden, W. Weng, J.A. Gladysz, Organometallics 11 (1992) 3635. (o) Y. Zhou, J.W. Seyler, W. Weng, A.M. Arif, J.A. Gladysz, J. Am. Chem. Soc. 115 (1993) 8509. (p) J.W. Seyler, W. Weng, Y. Zhou, J.A. Gladysz, Organometallics 12 (1993) 3802. (q) W. Weng, T. Bartik, J.A. Gladysz, Angew. Chem. Int. Ed. Engl. 33 (1994) 2199. (r) M. Brady, W. Weng, J.A. Gladysz, J. Chem. Soc. Chem. Commun. (1994) 2655. (s) W. Weng, T. Bartik, M. Brady, B. Bartik, J.A. Ramsden, A.M. Arif, J.A. Gladysz, J. Am. Chem. Soc. 117 (1995) 11922. (t) T. Bartik, B. Bartik, M. Brady, R. Dembinski, J.A. Gladysz, Angew. Chem. Int. Ed. Engl. 35 (1996) 414. (u) M. Brady, W. Weng, Y. Zhou, et al., J. Am. Chem. Soc. 119 (1997) 775. (v) S.B. Falloon, W. Weng, A.M. Arif, J.A. Gladysz, Organometallics 16 (1997) 2008. (w) V.W.-W. Yam, V.C.-Y. Lau, K.-K. Cheung, Organometallics 15 (1996) 1740. **Rh**, **Ir**: (x) T. Rappert, O. Nürnberg, H. Werner, Organometallics 12 (1993) 1359. (y) O. Gevert, J. Wolf, H. Werner, Organometallics 15 (1996) 2806. (z) H.B. Fyfe, M. Mlekuz, D. Zargarian, N.J. Taylor, T.B. Marder, J. Chem. Soc. Chem. Commun. (1991) 188. (aa) B.J. Stang, R. Tykwinski, J. Am. Chem. Soc. 114 (1992) 4411.

[4] See ref. ([3]j–v). See also, D. Astruc, Acc. Chem. Res. 30 (1997) 383.

[5] G.A. Somorjai, Introduction to Surface Chemistry and Catalytsis, Wiley, New York, 1994.

[6] (a) M. Akita, Y. Moro-oka, Bull. Chem. Soc. Jpn. 68 (1995) 420. (b) M. Akita, M. Terada, S. Oyama, Y. Moro-oka, Organometallics 9 (1990) 816. (c) M. Akita, M. Terada, S. Oyama, S. Sugimoto, Y. Moro-oka, Organometallics 10 (1991) 1561. (d) M. Akita, M. Terada, M., Y. Moro-oka, Organometallics 10 (1991) 2961. The reaction mechanism has been corrected in ref. ([6]k). (e) M. Akita, M. Terada, Y. Moro-oka, Organometallics 11 (1992) 1825. (f) M. Akita, M. Terada, Y. Moro-oka, Organometallics 11 (1992) 3469. (g) M. Akita, S. Sugimoto, M. Tanaka, Y. Moro-oka, J. Am. Chem. Soc. 114 (1992) 7581. (h) M. Akita, S. Sugimoto, A. Takabuchi, M. Tanaka, Y. Moro-oka, Organometallics 12 (1993) 2925. (i) M. Akita, N. Ishii, A. Takabuchi, M. Tanaka, Y. Moro-oka, Organometallics 13 (1994) 258. (j) M. Akita, M. Terada, N. Ishii, H. Hirakawa, Y. Moro-oka, J. Organomet. Chem. 473 (1994) 175. (k) M. Akita, A. Takabuchi, M. Terada, N. Ishii, M. Tanaka, Y. Moro-oka, Organometallics 13 (1994) 2516. (l) M. Akita, H. Hirakawa, M. Tanaka, Y. Moro-oka, J. Organomet. Chem. 485 (1995) C14. (m) M. Akita, H. Hirakawa, K. Sakaki, Y. Moro-oka, Organometallics, 14 (1995) 2775. (n) M. Terada, Y. Masaki, M. Tanaka, M. Akita, Y. Moro-oka, J. Chem. Soc. Chem. Commun. (1995) 1611. (o) M. Akita, S. Kato, M. Terada, Y. Masaki, M. Tanaka, Y. Moro-oka, Organometallics 16 (1997) 2392. **C4 complexes**: (p) M. Akita, M.-C. Chung, A. Sakurai, S. Sugimoto, M. Terada, M. Tanaka, Y. Moro-oka, Organometallics 16 (1997) 4882. **C1 complex**: (q) Y. Takahashi, M. Akita, Y. Moro-oka, J. Chem. Soc. Chem. Commun. (1997) 1557.

[7] (a) J.L. Davidson, Comprehensive Organometallic Chemistry, vol. 4, E.W. Abel, F.G.A. Stone, G. Wilkinson (Eds.), Pergamon, Oxford, UK, 1982, ch. 31–5. (b) M. Akita, Comprehensive Organometallic Chemistry II, vol. 7, E.W. Abel, F.G.A. Stone, G. Wilkinson (Eds.), Pergamon, Oxford, UK, 1995, ch. 4.

[8] (a) E. Sappa, A. Tiripicchio, P. Braunstein, Chem. Rev. 83 (1983) 203. (b) P.R. Raithby, M.J. Rosales, Adv. inorg. Chem. Radiochem. 29 (1985) 170. (c) R. Nast, Coord. Chem. Rev. 47 (1982) 89.

[9] D.F. Shriver, H.D. Kaesz, R.D. Adams, The Chemistry of Metal Cluster Complexes, VCH, New York, 1990.

[10] Halet et al. ([2]a) pointed out a possibility of interconversion between the 66e species **5** and the 68e permetallated ethene-type structure by addition and removal of a 2e-donor. But we could not get any evidence for formation of 68e species because of the failure in isolation of characterisable products.

[11] K. Yasufuku, K. Aoki, H. Yamazaki, Bull. Chem. Soc. Jpn. 48 (1975) 1616.

[12] G.A Kousantonis, J.P. Selegue, J.-G. Wang, Organometallics 11 (1992) 2704.

[13] T. Weidmann, V. Weinrich, B. Wagner, C. Robl, W. Beck, Chem. Ber. 124 (1991) 1363.

[14] $(\eta^5\text{-}C_5H_5)_2Mo_2(CO)_4$-system can be raised as a typical example. (a) R.J. Klinger, W. Butler, M.D. Curtis, J. Am. Chem. Soc. 98 (1975) 4645. (b) M.D. Curtis, Polyhedron 6 (1987) 759. (c) M.J. Winter, Adv. Organomet. Chem. 29 (1989) 101.

[15] L.S. Farrugia, S.E. Rae, Organometallics 11 (1992) 196.

[16] G.L. Geoffroy, S.L. Bassner, Adv. Organomet. Chem. 28 (1988) 1.

[17] G.W. Parshall, S.D. Ittel, Homogeneous Catalysis, Wiley, New York, 1992, p. 206.

[18] R.B. King, Organometallic Syntheses, vol. 1, Academic, New York, 1965, p. 93.

[19] International Tables for X-ray Crystallography, vol. 4, Kynoch Press, Birmingham, 1975.